RESEARCH ARTICLE | MARCH 15 1991

Dynamics of the ultraviolet photochemistry of water adsorbed on Pd(111)

M. Wolf; S. Nettesheim; J. M. White; E. Hasselbrink; G. Ertl

J. Chem. Phys. 94, 4609–4619 (1991)
https://doi.org/10.1063/1.460589

Dynamics of the ultraviolet photochemistry of water adsorbed on Pd(111)

M. Wolf, S. Nettesheim, J. M. White,[a] E. Hasselbrink, and G. Ertl
Fritz-Haber-Institut der Max-Planck-Gesellschaft, Faradayweg 4-6, D 1000 Berlin 33, Germany

(Received 30 May 1990; accepted 13 December 1990)

UV-laser irradiation ($h\nu = 6.4$ eV and 5.0 eV) of the water bilayer adsorbed on a Pd(111) surface leads to molecular desorption and to conversion of the adsorbed state as manifested in thermal desorption spectra. The latter effect is attributed to photodissociation of water on the surface. Time-of-flight measurements show that water molecules desorb with a translational energy of about 600 K for both photon energies indicating a nonthermal process. While desorption is largely suppressed with adsorbed multilayers, conversion within the first layer still proceeds. The dependence of the desorption yield on angle of incidence and polarization of the light reveals substrate excitations as the dominant primary step. A strong variation of cross sections with isotopic substitution is observed. This is interpreted as evidence for the operation of a mechanism involving excitation onto an isotope-independent excited potential energy surface followed by rapid deexcitation to the ground state so that, of the total number of species excited, only a small mass dependent fraction actually fragments or desorbs.

I. INTRODUCTION

During the last few years, photochemistry at the gas-metal interface has attracted considerable attention and rapidly advanced to a prolific new field.[1-3] But still our understanding of the basic mechanisms is limited.[4] In part, this arises, because of the strong coupling of excited states of molecules to the near-surface bulk electrons leading to rapid quenching through nonradiative excitation transfer to the substrate. Although it has long been believed that this would largely inhibit nonthermal chemical processes, it has recently been shown that excitations in the valence band regime ($h\nu < 10$ eV) can compete with the quenching thus resulting in photochemistry with significant cross sections. Among others, the photochemistry of the methylhalides,[5,6] of nitric oxide,[7-9] of nitrous dioxide,[10] of dioxygen,[11-13] and of metal hexacarbonyls[14-16] belong to the increasing body of experimental studies.

In order to obtain more information about the mechanistic aspects of surface photochemistry, we have investigated H_2O on Pd(111) with particular attention given to the effects arising upon isotope substitution. As we will show, these results demonstrate the close relationship of these processes to electron stimulated desorption (ESD), which is commonly discussed in the framework of the Menzel-Gomer-Redhead (MGR) model.[17]

Water adsorbed on metals has been studied in some detail,[18] but no studies have been done so far on Pd(111). On transition metal surfaces (like Pt, Pd, Ru, Ir), water bonds molecularly through the oxygen atom to the surface.[19,20] H_2O is a weakly chemisorbed species with a typical binding energy of 0.4 to 0.7 eV. A three dimensional structure is formed by hydrogen bonding, because the hydrogen bonding energy between two H_2O molecules is energetically competitive to the molecule-substrate bond. The O-O distance in the hexagonal ice structure is comparable to the metal atom-atom distance on hexagonal surfaces. On Pd(111) only a slight compression of 6% is necessary to form an epitaxial structure. In this structure, called the *water bilayer*, water molecules are hydrogen bonded in hexagonal rings such that alternating molecules have their lone pairs in the direction towards the substrate. The others are raised by ~ 1 Å from the surface.[21,22] The saturation coverage of this structure is 2/3 ML referring to the number of metal atoms on the surface. Within this structure the gas phase molecular bond angle, bond length, and force constants are only slightly perturbed upon adsorption. Because of the high surface diffusion rate, clusters of this type are even formed at fractional monolayer coverages.[23]

This well known structure and properties of adsorbed water together with the transparency of water vapor[24] and solid ice[25,26] for near UV radiation (Fig. 1) make the water-metal system a promising candidate for surface photochemical studies, because it can be expected that surface effects can be clearly isolated from bulk effects and that a more detailed picture of the electronics of surface photochemistry evolves.

Photodesorption and dissociation of thick condensed H_2O films has been studied by Nishi *et al.*[27] with the essential

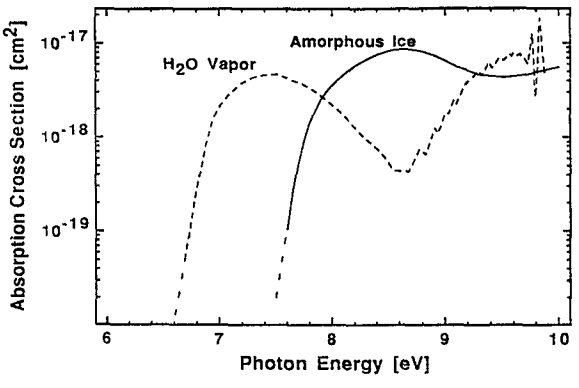

FIG. 1. Absorption spectrum of water and amorphous ice. In the range of photon energies used in this work both are practically transparent. Compiled from Refs. 24-26.

[a] Permanent address: Dept. of Chemistry, University of Texas, Austin, TX 78712, USA.

 0021-9606/91/064609-11$03.00

finding that desorption of H_2O was only observable as two photon process with 5.0 eV radiation at intensities exceeding 10 MW/cm^2.

The present study concentrates on the photochemistry in the first layer adsorbed on a metal and applies much weaker intensities. A brief report has been published recently.[28] Here we present extended results detailing cross sections for the photochemical processes observed. Further we report time-of-flight spectra of desorbed H_2O and a polarization study identifying the initial excitation steps leading to photodesorption. Especially, we report and discuss marked isotope effects in cross sections.

II. EXPERIMENTAL

The UHV apparatus used for this experiment has been described in detail elsewhere.[10] It was equipped with low-energy electron diffraction and Auger electron spectroscopy (LEED/AES) facilities, an Ar^+ sputter gun, and a quadrupole mass spectrometer (QMS), which could be rotated around the sample. Ar^+ bombardment and repeated oxidation cycles at 800 K surface temperature were used to clean the Pd(111) surface until no impurities were detectable by AES and no CO desorption could be monitored accompanying oxygen TDS.

Water was dosed using a pulsed molecular beam. Distilled water was kept in a reservoir consisting of two connected glass ampoules. In order to remove dissolved impurities and gases, the water was distilled several times between the two ampoules while pumping the reservoir through the operating pulsed nozzle.

The molecular beam was formed by immersing the water reservoir into an ice bath and bubbling Ar (Linde, 99.998%) with a backing pressure of 1.5 bar through the liquid. The connecting pipes and the nozzle itself were kept at 50 °C in order to avoid condensation. Under these conditions, the molecular beam consisted of 10% H_2O and 90% Ar.

D_2O used for the isotope effect experiments had a purity of 99.7% (Carl Roth KG). By seeding it in He (Messer–Griesheim, 99.999%) and using the QMS to detect mass 17, an upper limit of 5% for the presence of H_2O could be established.

The Pd(111) crystal was typically held at 95 K surface temperature during irradiation. Preparation of the water bilayer was done by dosing at 145 K surface temperature in order to avoid the buildup of multilayers. Line-of-sight thermal desorption spectra (TDS) were recorded at a heating rate of 3 K/s. The sample was irradiated with pulsed UV light from an excimer laser (Lambda Physik, EMG 150 MSC) that outputs 6.4 eV (193 nm) radiation when filled with ArF gas mixture and 5.0 eV (248 nm) when run with KrF. Pulse duration is 13 ns and 17 ns full width at half maximum (FWHM) for ArF and KrF, respectively. If not otherwise noted, the sample was uniformly irradiated at normal incidence using unpolarized light. The laser light could be polarized using a Rochon prism. In order to avoid substantial thermal heating due to absorbed light, the laser fluence impinging the surface was kept below 5 mJ/cm^2 per pulse, which results in a calculated transient temperature rise of less than 15 K.[29]

The yield of desorbing H_2O molecules initiated by a laser pulse was monitored with the QMS set at a certain desorption angle, typically 23 °, with respect to the surface normal. With this setup, it was also possible to record time-of-flight (TOF) spectra employing a digital storage oscilloscope (Tektronix 2432A) for time resolved recording and shot-to-shot averaging. A crystal-to-ionizer distance of 50 mm was used. The data were corrected for the flight time through the QMS, which had been determined in a calibration experiment to 8 μs. For data analysis, the spectra were fitted by a modified Maxwell–Boltzmann distribution[30]

$$n(t) = at^{-4}\exp\left[-b\left(\frac{d}{t}-v_0\right)^2\right], \tag{1}$$

where a is a normalization constant, b a measure of the translational energy, v_0 an offset flow velocity, and d the distance between the sample and the detection volume. The velocity, v, is connected to the flight distance and flight time by $v = d/t$. The flux weighted average velocity, $\langle v\rangle$, and translational energy, $\langle E_{\text{trans}}\rangle$, are then derived from the fit curve by numerical integration.

III. RESULTS

A. Thermal desorption spectroscopy

Figure 2 shows a series of TD spectra after increasing doses of H_2O at 95 K surface temperature. For a low dose, desorption occurs with maximum rate around 165 K. With increasing coverage the desorption maximum shifts towards higher temperatures indicating first order desorption with lateral attraction.[31] Upon saturation of this state a second

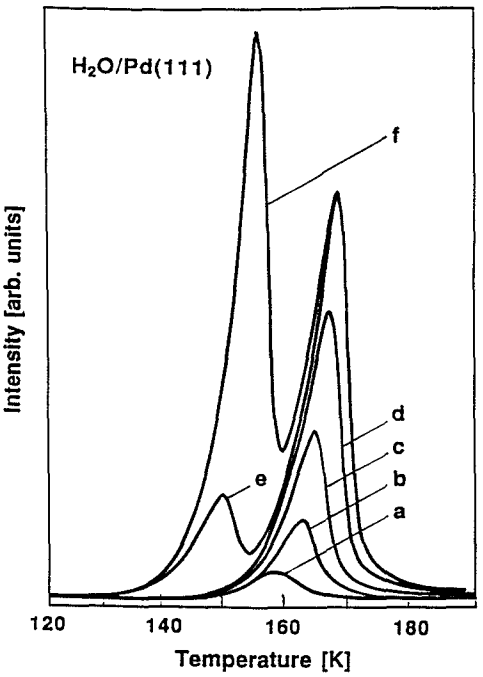

FIG. 2. TD spectra as function of dose (a) $\theta = 0.04$ ML, (b) 0.1 ML, (c) 0.3, (d) 0.5 ML, (e) 0.8 ML, (f) 1.5 ML, with $\theta = 0.66$ corresponding to the maximal area of the bilayer peak). After saturation of the bilayer amorphous ice grows which desorbs at 150 K.

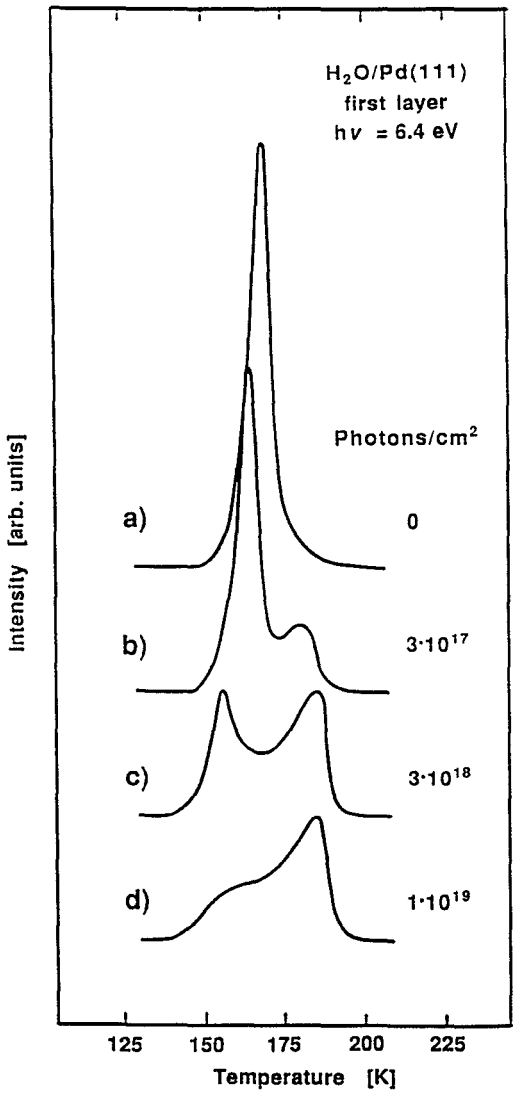

FIG. 3. Thermal desorption spectra of the water bilayer (a), after irradiation with 0.3×10^{18}, 3×10^{18}, and 10×10^{18} photons/cm^2 ($h\nu = 6.4$ eV) [(b) to (d)].

one grows which desorbs above 150 K. With an increasing dose, the coverage in this state does not saturate which is clear evidence for multilayer growth by sublimation of ice.

These observations are analogous to those made on other transition metals. The first binding state is identified as the H_2O bilayer. Presumably, this structure is also formed even at very low coverages. The multilayer will most probably be formed as amorphous ice.

Upon UV irradiation of the bilayer ($h\nu = 6.4$ eV) conversion into a new desorption feature with a maximum at 185 K is observed (Fig. 3). The integrated area of this new feature saturates after irradiation with $3\cdot10^{18}$ photons/cm^2. The saturation value is 45% of the initial H_2O coverage. In parallel, the peak desorption temperature of the residual water decreases approaching the desorption temperature of multilayer ice. With continuing irradiation, the integrated area of this feature decreases. From the decrease of the total TDS area, it is evident that desorption must also occur in part during irradiation, which can indeed be monitored directly using the QMS. Only desorption of H_2O was observed, i.e., no desorption of fragments (OH, H) was detectable within the background resulting from cracking of H_2O. This sets an upper limit that less than 5% desorb as fragments.

TDS of the irradiated bilayer also shows, at higher temperatures, desorption of O_2 from atomic O recombination as well as some H_2, but Pd bears some experimental obstacles on quantitative detection of these adsorbates because both dissolve readily into the subsurface region.

A similar H_2O desorption feature at 185 K is known in the literature to occur for atomic oxygen coadsorbed with H_2O.[32] In order to demonstrate this also for the present system, H_2O has been adsorbed after predosing about 0.05 ML of atomic oxygen at 300 K. Under these conditions, the TD spectrum shown in Fig. 4(b) is observed which resembles the one obtained after irradiating the H_2O bilayer with $3\cdot10^{18}$ photons/cm^2 and subsequently redosing 0.3 ML of H_2O [Fig. 4(c)]. It has been established by EELS studies on

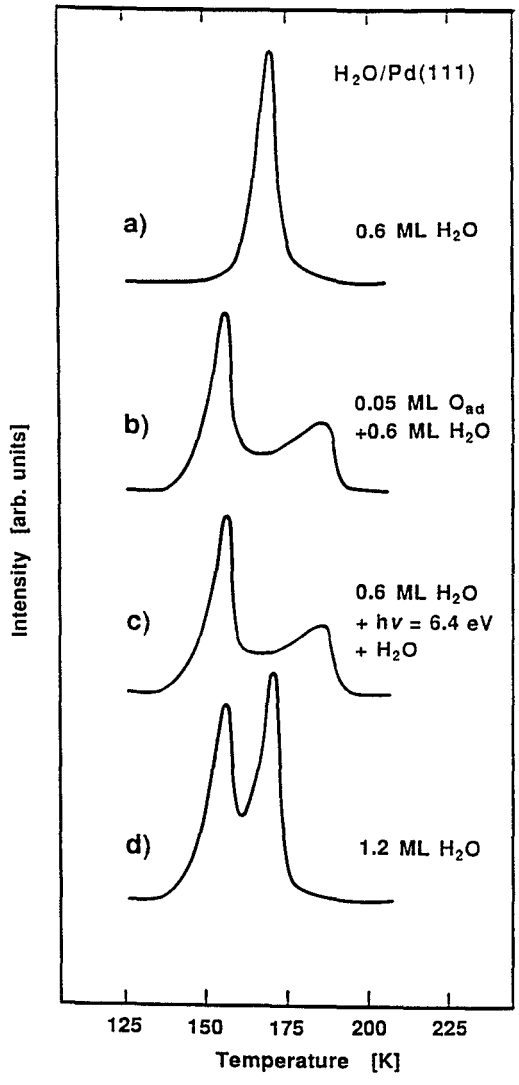

FIG. 4. Thermal desorption spectra of the water bilayer (a), of H_2O coadsorbed with 0.05 ML of atomic oxygen (b). If the bilayer is irradiated with 3×10^{18} photons/cm^2 and afterwards redosed by 0.3 ML of H_2O trace (c) is obtained. Trace (d) shows the multilayer and bilayer desorption peak indicating the close desorption temperatures of the multilayer and the residual water in the case of the irradiated layer.

Pt(111)[33] and Pd(100[34,35] that water coadsorbed with atomic oxygen reacts above 150 K to form hydroxyl groups, $H_2O_{ad} + O_{ad} \rightarrow 2OH_{ad}$, which only recombine at higher temperatures (185 K) leading again to the release of water into the gas phase and to atomic oxygen retained on the surface, $2OH_{ad} \rightarrow H_2O + O_{ad}$.

It is therefore suggested to attribute the TDS peak at 185 K, seen after irradiation, to a recombination of hydroxyl groups which must result from photolysis of adsorbed water by the UV light. However, at present, we can not establish whether hydroxyl groups are the primary photolysis product or if they are produced thermally during TDS from other primary photolysis products, for example, from atomic oxygen and H_2O. Also atomic oxygen left from OH recombination ($2OH_{ad} \rightarrow H_2O + O_{ad}$) might react with photolytically produced hydrogen and contribute to the H_2O desorption at 185 K. Regardless, it can be concluded that recombination of photolysis products is the process dominating the TDS feature at 185 K. In the following we will call it *conversion process*, because the state of the adsorbate has not been directly established yet.

B. Time-of-flight spectroscopy

Time-of-flight spectra have been recorded for H_2O desorbed with 6.4 and 5.0 eV radiation and for D_2O with 6.4 eV radiation. In order to improve the resolution, only a 6 mm wide vertical stripe of the crystal was illuminated. Starting with the saturated bilayer the signals from the first 256 laser shots ($0.6 \cdot 10^{18}$ photons/cm^2) have been accumulated. In order to improve the statistics, multiple sets of so obtained data were averaged. No shift of the maximum in the time-of-flight spectrum with the change of the composition of the layer and its depletion was found.

The TOF spectrum of H_2O, desorbed at $h\nu = 6.4$ eV [Fig. 5(a)] can be fitted by a single modified Maxwell–Boltzmann distribution (Eq. 1). This evaluation yields an average translational energy $\langle E_{trans} \rangle$ of 104 ± 5 meV. This value would correspond to a temperature, $\langle E_{trans} \rangle / 2k$, of 600 K, which is 500 K in excess of the actual surface temperature clearly demonstrating the nonthermal (i.e., photochemical) character of the desorption process. In contrast to other systems,[7-9] where a slow (i.e., "thermal") desorption channel was also observed frequently, there is no indication of such a feature in this system. For 5.0 eV photon energy the signal is much smaller due to a smaller cross section, which is apparent in the noise on the curve in Fig. 5(b), but still can be fitted with reasonable accuracy. With these precautions in mind $\langle E_{trans} \rangle$ is 94 ± 15 meV, i.e., within the error limits identical to the value for 6.4 eV radiation.

For D_2O the same procedure provides a TOF spectrum [Fig. 5(c)] whose evaluation yields an average translational energy $\langle E_{trans} \rangle$ of 100 ± 7 meV, practically equal that for H_2O. The mean velocities, $\langle v \rangle$, are 900 ± 40 m/s for D_2O and 975 ± 25 m/s for H_2O. The ratio, 1.08 ± 0.06, is to be compared to the square root of the mass ratio, 1.05, to which it agrees within the experimental error.

For H_2O and $h\nu = 6.4$ eV, the dependence of the desorption yield on the laser fluence per pulse has been tested over a wide range (Fig. 6). Between 2 and 40 mJ/cm^2, the dependence is entirely linear indicating that the process discussed here originates from a single photon excitation. For higher fluences (≈ 85 mJ/cm^2) a much higher desorption yield is observed which is consistent with the expectation of substantial thermal desorption at these laser fluences when the transient temperature during the laser pulse (≈ 350 K) is well above the thermal desorption temperature in TDS.

The angular distribution of H_2O desorbed by 6.4 eV radiation from the bilayer has been recorded by rotating the QMS around the crystal (Fig. 7). For this measurement the angle of incidence of the laser light had to be set to 23 ° with

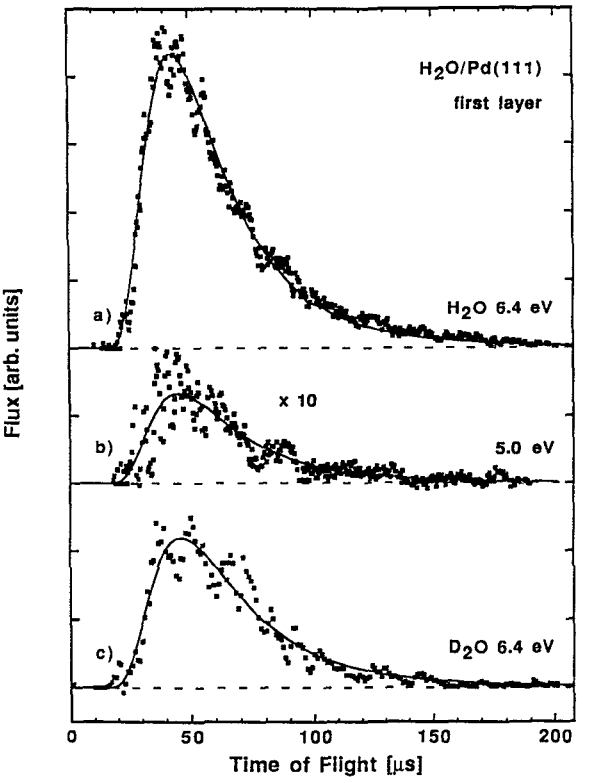

FIG. 5. Time-of-flight (ToF) spectra for H_2O/D_2O desorbed from Pd(111). The spectrum for 5.0 eV excitation has been enlarged by a factor of 10. The flight distance is 50 mm. The observed mean translational energy, $\langle E_{trans} \rangle$, is in all cases about 100 meV.

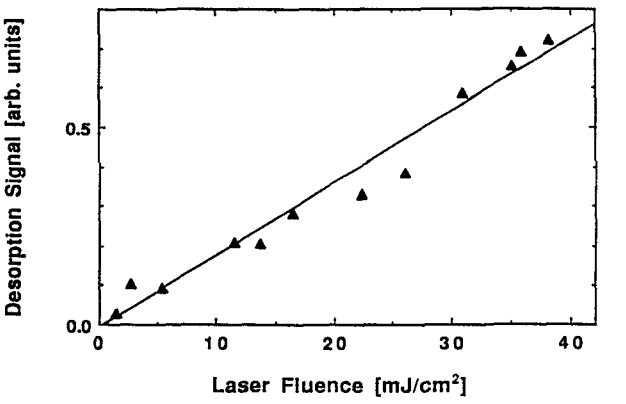

FIG. 6. Dependence of the desorption yield on laser fluence. Up to 40 mJ/cm^2 the dependence is linear indicating that a single photon process initiates desorption.

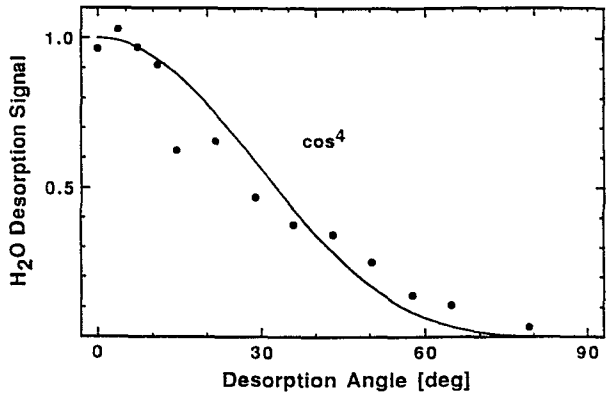

FIG. 7. Angular distribution of H_2O molecules desorbed by 6.4 eV radiation. The solid curve gives a $\cos^4$ distribution for comparison.

respect to the surface normal. The curve obtained is best represented by a $\cos^4$ function.

C. Cross sections

The cross sections for the conversion and desorption process were determined from a series of TD spectra obtained after irradiating the bilayer with varied photon fluences. We will define the cross sections from the experimentalists point of view in the most direct and useful way, by referring to the incident fluence. Any other definition, e.g., the sum of incident and multiply reflected or only the absorbed fluence, would already imply an interpretation of the process. The photochemical cross section multiplied by the photon fluence gives the fraction of surface species which undergo chemical transformation or when multiplied by the surface coverage gives the quantum yield.

The number N_{con} of converted H_2O molecules saturates exponentially with the number of photons n_{ph} irradiating the surface as

$$N_{\text{con}} = N_{\text{con,max}}\left[1 - e^{-\sigma_{\text{con}} n_{\text{ph}}}\right]. \tag{2}$$

The number of converted molecules has been determined from the integrated area of the conversion peak in a series of TD spectra as a function of photon fluence (Fig. 8). $N_{\text{con,max}}$

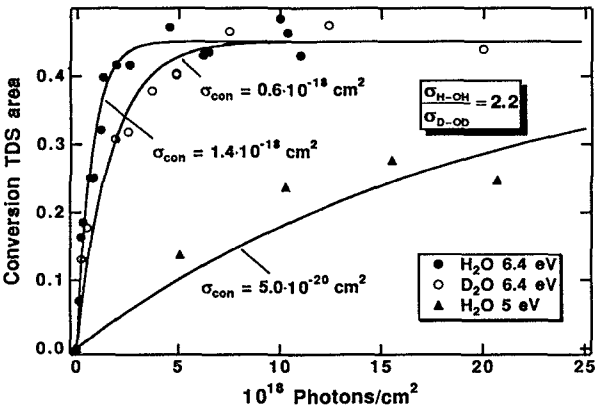

FIG. 8. Buildup of the conversion feature in TDS vs photon fluence. The cross section for 6.4 eV radiation (●) is by a factor of 24 larger than for 5.0 eV (▲). At 6.4 eV the cross section for D_2O (○) is by a factor of 2.2 smaller than for H_2O.

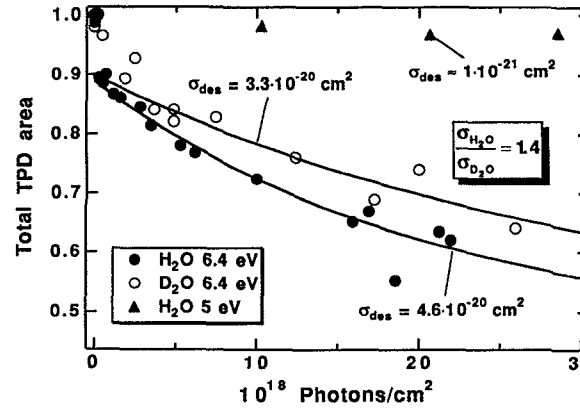

FIG. 9. Depletion of the total H_2O TDS area vs photon fluence. The tail, when the conversion feature is saturated, has been fitted by an exponential decay ansatz. The cross section for 6.4 eV radiation (●) is by at least a factor of 25 larger than for 5.0 eV (▲), but in both cases smaller than for the conversion process. For 5.0 eV irradiation more point at higher photon fluences than shown have been evaluated. For D_2O (○) the cross section is smaller by a factor of 1.4.

is 45% of the initial H_2O coverage. This evaluation yields cross sections σ_{con} of $1.4(\pm 0.1)\times 10^{-18}$ cm² and $5.0(\pm 0.7)\times 10^{-20}$ cm² for 6.4 eV and 5.0 eV irradiation, respectively.

The depletion of the total H_2O–TDS area (Fig. 9), which is due to photonstimulated desorption, can be represented by an exponential decay which approaches asymptotically the saturation TDS area of the conversion feature $N_{\text{con,max}}$.

$$N = (N_{\text{max}} - N_{\text{con,max}})e^{-\sigma_{\text{des}} n_{\text{ph}}} + N_{\text{con,max}}. \tag{3}$$

Evaluation of the data points for irradiations exceeding the saturation of the conversion feature yields desorption cross sections σ_{des} of $4.6(\pm 0.7)\times 10^{-20}$ cm² and $1(\pm 0.6)\times 10^{-21}$ cm² for 6.4 eV and 5.0 eV excitation, respectively. If the fitted curve for $h\nu = 6.4$ eV (Fig. 9) is extrapolated to zero irradiation, it does not go through one. About 10% of the water coverage is missing from this extrapolation. This indicates that desorption plus the 185 K conversion peak, by themselves, cannot account for all of the initial water. The extra loss of water occurs during the same irradiation period in which the conversion features grows. This is consistent with the expectation that not all photofragments will recombine and desorb as H_2O which is also indicated by the observation of atomic O on the surface after flashing to 200 K. Additional measurements recording the decay of the desorption signal with the QMS, support the desorption cross section derived from TDS.

The cross sections of both processes (i.e., conversion and desorption) have also been determined for deuterated water, D_2O, for 6.4 eV irradiation. The conversion cross section σ_{con} is reduced to $6.0(\pm 0.7)\times 10^{-19}$ cm² (Fig. 8) and the desorption cross section σ_{des} to $3.3(\pm 0.2)\times 10^{-20}$ cm² (Fig. 9), i.e., the ratio of the cross sections for H_2O and D_2O is 2.2 and 1.4 for conversion and desorption, respectively. Although the given absolute cross sections might have large systematic errors, the relative values should be accurate

within 10%. These isotope effects will be discussed in the framework of the MGR model in the discussion section.

D. Dependence on the polarization of the radiation

The dependence of the yield of a photochemical process on polarization and angle of incidence of the stimulating light can be used to discriminate between processes which originate from direct light absorption in the substrate–adsorbate complex and those which are driven by substrate (bulk) excitations.[10] The physical reason for this is that in the first case the electric field interacts with localized orbitals, whereas in the second case absorption is governed by the properties of the solid.

From the published values of the index of refraction of Pd[36] the absorption by the substrate can be calculated based on Fresnel's formula.[37] Because the penetration depth of the light is not strongly dependent on the angle of incidence a constant fraction of the generated excited hot carrier is expected to interact with the adsorbate. Therefore, the dependence on angle of incidence and polarization should mainly be governed by the absorption. Additionally, the electric field components normal and parallel to the surface can be calculated.[38] The experimentally observed dependence of the yield on polarization and angle of incidence can then be compared to both the predictions based on absorption by the solid as well as with the expectations based on the surface electric fields which would interact with the transition dipole in the case of a localized excitation in the substrate–adsorbate complex. For further details the reader is referred to Ref. 10.

In the following we will focus on the desorption channel, but the conversion feature exhibits the same dependence as was checked for three angles. Measurements of the desorption signal were performed switching between *s*- and *p*-polarization at various angles of incidence. The mass spectrometer used for detection was simultaneously rotated with the crystal in order to keep the detection geometry fixed. Starting with the saturated bilayer the desorption signal was recorded over time. The data were then extrapolated to zero irradiation to obtain the initial desorption yield as well as fitted to obtain a cross section. Both procedures yield practically identical results and avoid misleading results due to the varying rate of coverage depletion. The obtained initial desorption yields are plotted in Fig. 10 together with the ratios of the data points which will be useful for the following discussion. The shown error bars represent the standard deviation resulting from two to four independent measurements.

Good agreement of the experimental findings with the predictions of the bulk absorption model is found. In particular, the occurrence of the maximum at 50 ° for *p*-polarization and the agreement of the measured ratios should be noted. With respect to the model of direct excitation it is found that the data can neither be reconciled with a transition dipole which is purely in the plane of surface nor one which is normal to it. From the experimentally observed signal at 0 ° it is obvious that the inplane component should contribute and from the observed maximum at 50 ° that the normal component should also contribute. From the structure of the water bilayer it can be concluded that there

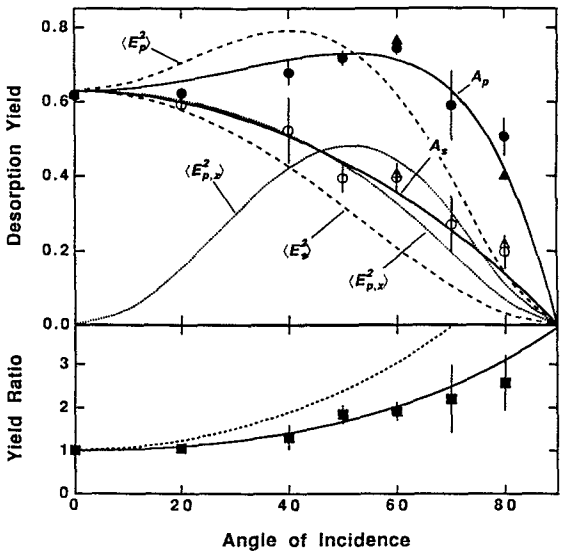

FIG. 10. H_2O desorption yield as function of polarization (*s*: ○ and *p*: ●) and angle of incidence of the light ($h\nu = 6.4$ eV). Also shown are data for the conversion process (*s*: △ and *p*: ▲). Within the error bars the data can only be described by a model which is based on absorption in the metal substrate as primary excitation step (solid curves; *s*: A_s and *p*: A_p). The best obtainable fit within the direct absorption model is indicated by the dashed lines (*s*: $\langle E_s^2 \rangle$ and *p*: $\langle E_p^2 \rangle = \langle E_{p,x}^2 \rangle + 2/3^* \langle E_{p,z}^2 \rangle$). The dotted lines give the individual field components, inplane $\langle E_{p,x}^2 \rangle$ and normal $\langle E_{p,z}^2 \rangle$, for *p* polarization. (The corresponding curves in Fig. 18 of Ref. 10 are in error.) The lower panel shows the ratios of the desorption data (■) and curves in the upper panel. The experimental data as well as the curves for the electrical field strength have been normalized to the absorption curves at 0 °.

should be no strong preference of any direction within the surface plane, which is further corroborated by the identical results, within 3%, obtained at 0 ° for *s*- and *p*-polarization. An attempt was made to fit the data with a mixture of the inplane and normal component. The best results were obtained when 2/3 of the normal field strength were added to the inplane field. This could be interpreted as a net transition dipole moment inclined 60 ° from the surface normal and azimuthally distributed with the sixfold symmetry of the substrate. But the fit is far from satisfactory. The maximum occurs at too small an angle and at large angles the calculated yield ratios are too high and well above the experimental error.

We conclude that the observed desorption channel data can not be explained with any simple model involving only direct excitation of the adsorbate–substrate complex. But it is easily reconciled by a model involving bulk excitations as the dominant primary excitation step. The data obtained for the growth of the conversion features at three angles, 0 °, 60 °, and 80 ° (Fig. 10) shows practically the same dependence indicating that here, bulk excitations also dominate. Similar data were found in our studies on N_2O_4 dissociation[10] and O_2 desorption.[13] This agreement further supports the conclusion that substrate excitations are in many cases the initial step stimulating the observed photochemistry.

E. Coverage dependence

For both desorption and conversion we have studied the yield as a function of H_2O coverage (Fig. 11). In the sub-

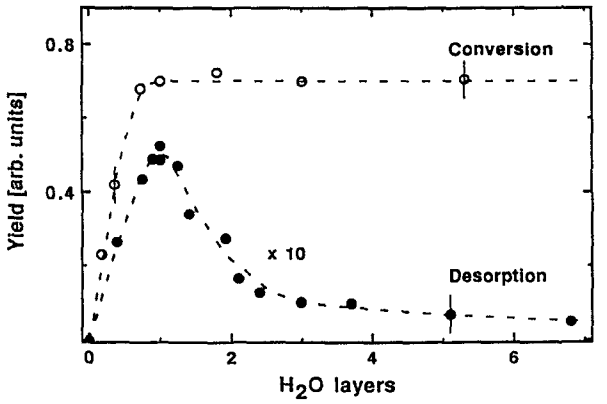

FIG. 11. Desorption (■) and conversion (□) yield vs H_2O coverage ($h\nu = 6.4$ eV). The desorption yield has been multiplied by a factor 10. The lines are drawn to guide the eye. One H_2O layer corresponds to the saturation coverage of the bilayer (0.66 ML).

monolayer regime, both yields increase linearly with coverage. The conversion yield starts to saturate when the coverage exceeds 60% of the bilayer saturation coverage (0.66 ML). This corresponds to the situation when nearly all adsorbed water molecules (apart from the smaller fraction which desorbs during conversion) are channeled into the conversion feature. With increasing coverage the initial desorption yield increases until the bilayer is saturated, but then it decreases rapidly and levels off at 4–5 ML coverage at only 10% of the maximum yield. Adsorption of a second layer of H_2O already decreases the desorption yield by a factor of two. It has to be kept in mind that amorphous ice grows as microcrystals and not layer-by-layer. Therefore, we expect part of the first layer to be exposed to the vacuum even for total coverages exceeding 2 ML so that some desorption from the first layer still occurs undisturbed.

For both processes, a high propensity for the first adsorbed layer is obvious. Dissociation in the first layer proceeds even with adsorbed multilayers because of the transparency of amorphous ice for the UV radiation used in this study. If multilayers are adsorbed desorption is much less effective since these prevent the escape of molecules from the first layer. Desorption from the multilayers themselves is at least by an order of magnitude less efficient.

In TOF spectroscopy the striking observation has been made that the average translational energy, $\langle E_{\text{trans}} \rangle$, is strongly dependent on coverage. With increasing coverage $\langle E_{\text{trans}} \rangle$ continuously decreases from initially 100 to 68 meV for 1–7 H_2O layer (0.66–4.4 ML) coverage, respectively. This is shown in the inset of Fig. 12 and becomes directly obvious from the position of the maximum in the TOF spectra.

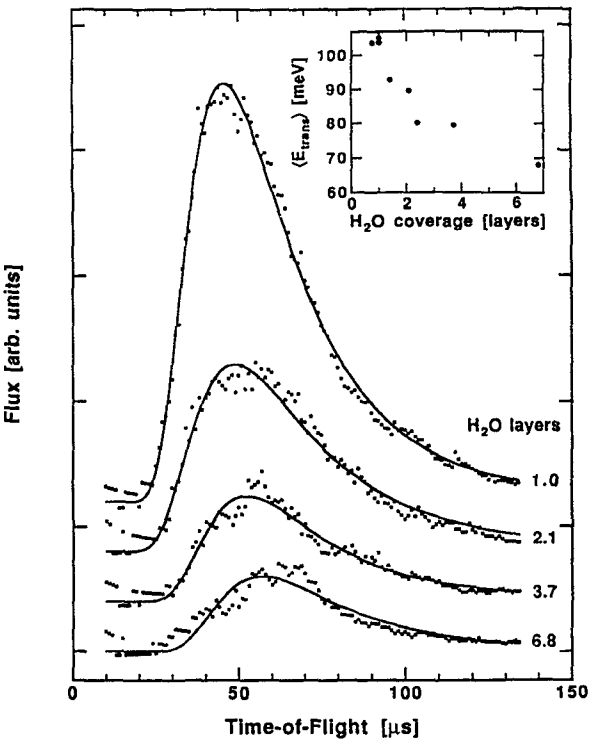

FIG. 12. Time-of-flight spectra of desorbed H_2O for different coverages ($h\nu = 6.4$ eV). The mean translational energy $\langle E_{\text{trans}} \rangle$ decreases from 105 meV for 1 layer to 68 meV for 6.8 H_2O layers coverage (inset).

IV. DISCUSSION

A. Summary of photochemical processes observed

The photochemical character of the processes studied is evident for several reasons: (i) The desorption yield is linear with laser fluence, whereas for a thermal process an exponential behavior above a threshold would be expected. (ii) The observed dependence on photon energy indicates that the quantum character of the photons is of importance and not only the net resulting absorbed power. (iii) The ToF spectra show nonthermal desorption.

Two processes are evident from our TDS data: (i) photodesorption of H_2O, and (ii) conversion due to photodissociation of H_2O with the fragments retained on the surface. At the present state our experimental data do not reveal whether atomic oxygen or hydroxyl groups are the primary photolysis products. At least two molecular processes are conceivable:

$$H_2O \rightarrow H + OH \tag{4a}$$

or

$$H_2O \rightarrow H_2 + O, \tag{4b}$$

but from energy considerations the first process appears to be more likely, because the gas phase threshold for the latter process is 9 eV.[39] Experiments using other techniques which directly characterize the photolysis products retained on the surface are being prepared in order to tackle this question. Conversion saturates with nearly 50% of the initial coverage in the new state. This might indicate that it is only possible to dissociate the lower layer of the bilayer structure. But, on the other hand, it can also arise from saturation of available sites for the photofragments.

The cross sections for both processes are listed in Table I. For both desorption and conversion the values for the 6.4 eV irradiation are larger, by an order of magnitude, than for the 5.0 eV irradiation. Their ratio is about 25 for both the buildup of the conversion feature and (within the relatively large error range due to the small cross section for $h\nu = 5.0$

TABLE I. Cross sections in 10^{-18} cm^2.[a]

	6.4 eV		5.0 eV
	H_2O	D_2O	H_2O
Desorption	0.046(± 0.007)	0.033(± 0.005)	0.001(± 0.0006)
Conversion	1.35(± 0.11)	0.60(± 0.07)	0.05(± 0.01)

[a] Errors are derived from the least-square-fit routine only and do not account for systematic errors.

eV) also for the desorption channel. The strong enhancement with increasing photon energy indicates an underlying electronic resonance mechanism for both processes. Because of the similar dependence on photon energy it is tempting to assume that both processes are stimulated by the same primary electronic excitation. The conversion has the larger cross section of the two processes. It saturates while desorption still proceeds. However, the obtained cross section has to be interpreted with caution. It describes how effectively H_2O molecules are converted into the new state and not *a priori* how effectively H_2O molecules are dissociated. Conversion could involve one dissociation event and a subsequent reaction of other water molecules. More complex structures with one dissociated molecule surrounded by one or several intact molecules would be built. For coadsorbed oxygen this effect is well known in the literature[21,40] and is apparent in our data from the small amount of coadsorbed atomic oxygen (0.05 ML) which is needed to reproduce the maximum coverage in the 185 K state, that can be formed photolytically. If conversion saturates due to limited availability of sites for the fragments a factor of the kind $(1 - [OH]/[OH]_{max})$ has to be included in the rate equation. Data analysis then yields conversion cross sections which are by a factor 1.8 smaller than the numbers given in Table I. But these problems would modify the derived numbers independent of photon energy and isotope composition. Therefore none of the drawn conclusions which are based on the relative cross sections, would be affected.

B. Mechanism

The dependence on polarization reveals that substrate excitations are the dominant primary excitation step. The excited substrate e^- (hot electron or photoelectron) may inelastically scatter or resonantly attach to an affinity level of the adsorbed water molecules. There have been many observations of dissociative negative ion formation by electron impact on gaseous H_2O.[41] These experiments show three resonances at 6.5, 8.6, and 11.8 eV electron energy, which have been correlated to the $^2B_1$, $^2A_1$, and $^2B_2$ state, respectively.[42]

Fisher *et al.*[43] found the highest occupied states of H_2O adsorbed on Pt(111) at 5.4, 8.2, and 11.9 eV ($1b_1$, $3a_1$, and $1b_2$) below the Fermi level. The respective values in ice are rather similar.[44] The lowest unoccupied levels of H_2O are the $4a_1$ and $2b_2$, with the latter being energetically lower.[45] We are not aware of any study detailing the energetic positions of these levels, but both probably lie between the Fermi and vacuum level. The large gap between the occupied and unoccupied states confirms that direct excitation of H_2O orbitals is not possible with our photon energies. Transfer of an excited bulk electron into one of the unoccupied antibonding orbitals of H_2O, on the other hand, is possible with the available photon energies. Occupation of the $4a_1$ orbital has been discussed in connection with the gas phase dissociative attachment processes.[46] We therefore believe that the photochemistry proceeds via a mechanism similar to dissociative electron attachment in gas phase. In the so formed excited H_2O^- state, transfer of energy into nuclear motion occurs until the electron is quenched back to the substrate. However, it will need further detailed knowledge of the electronic structure to identify firmly the states involved.

The work function of the clean Pd(111) surface is 5.5 eV.[47] We are not aware of any reported data on its change by water adsorption. A reduction of the work function is expected similar as reported for Pt(111)[43] (1.5 eV) and for Pd(100)[35] (0.4 eV). With the photon energies used in this study, excitation of electrons to empty levels below the vacuum level ("*hot electrons*") will occur, which may tunnel through the remaining low potential barrier. Excitation above the vacuum threshold ("*photoelectrons*") will be feasible for 6.4 eV and to a much lesser extent also possible for 5.0 eV photons. For 6.4 eV excitation the electron distribution will be significantly broader and extend to higher energies which might give rise to the higher cross sections in the latter case.

Both photochemical processes are most effective in the first layer of adsorbed water molecules. Photodesorption ceases with adsorbed multilayers, while photodissociation in the first layer still proceeds. These findings are strong evidence for a model where the primary processes are confined to the metal-adsorbate interface. Amorphous ice is transparent for the applied UV photons so that electron excitation at the metal-adsorbate interface can still proceed. But adsorbed multilayers prevent, on the other hand, the release of H_2O molecules into the gas phase. This conclusion is especially striking in view of the common argument on the strong quenching of electronic excitations in the close vicinity of a metal surface.

The explanation for this selectivity can be sought in two arguments: (i) The special structure of the bilayer and its electronic interaction with the substrate might be important, e.g., the necessary affinity level for electron transfer might only be available in this configuration. (ii) Electron transfer through the first water layer might be prohibited. Gilton *et al.*[48] have observed that water layers also prevent electron transfer into CH_3Cl multilayer adsorbed on-top, which is on the other hand effective on the chlorinated and Xe covered surface. However, they find that the attenuation length is 4 ML, that means larger than to fully account for the effects observed here. But still it might well indicate that electron capture or scattering by H_2O are rather efficient so that transfer into layers adsorbed on-top is suppressed. Also preliminary data on the photochemistry of the CO/H_2O coadsorption system points in that direction. In this system the typical bilayer structure is presumably not formed, but desorption is still effective.[49]

The observed surface selectivity of the water/Pd photochemistry clearly demonstrates that the adsorbate–substrate

interaction can open pathways in surface photochemistry which are neither present in gas nor condensed phase.

C. Interpretation of the isotope effect

The observed marked isotope effects can certainly not be attributed to electronic structure effects; e.g., it is known that the gas-phase dissociative electron attachment (DEA) resonances show only small ($\leqslant 100$ meV) isotope shifts.[50] These would certainly have been washed out in the adsorbed state. The isotope effect observed in DEA cross sections can be explained by life time arguments which are rather similar to what will be discussed in the following. Strong isotope effects have also been observed in ESD,[51,52] especially hydrogen desorption. These experiments proved the validity of the Menzel–Gomer–Redhead model.[53,54] The MGR model considers the following simple picture: excitation onto a repulsive potential energy curve at distance x_0 is followed by rapid deexcitation to the ground state, so that motion along the excited curve occurs only for a limited period of time. During this time potential energy is converted into translational energy, which, if the time is long enough, will be sufficient to escape the remaining well depth of the bound ground state; i.e., there will be a critical distance x_c so that the process (e.g., desorption) will only complete successfully, if motion on the excited potential curve occurs beyond it. Otherwise, if $x \leqslant x_c$, the particle is recaptured. This picture originally proposed for a repulsive excited state interaction holds also for an attractive interaction in which case the nuclei are displaced and deexcitation takes place onto the repulsive branch of the ground state potential (Antoniewicz model).[55]

The total probability of a successful completion of the fragmentation process, regardless of type, is then given by

$$P_d = \exp\left(- \int_{x_0}^{x_c} \frac{dx}{\tau v} \right), \tag{5}$$

where v is the velocity along the excited state curve and τ the lifetime with respect to deexcitation to the ground state. By expressing v in terms of the kinetic energy, we obtain

$$P_d = \exp\left(- \sqrt{\frac{m}{2}} \int_{x_0}^{x_c} \frac{dx}{\tau \sqrt{V(x_0) - V(x)}} \right), \tag{6}$$

where $V(x)$ is the excited state potential energy. Equation (6) contains the proper dependence on mass m. The observable total cross section σ_d is then given by

$$\sigma_d = P_d \cdot \sigma_{ex}, \tag{7}$$

where σ_{ex} is the excitation cross section. Particles differing in their isotope composition will experience practically identical potential curves and primary excitation cross sections as well as lifetimes, but have different masses and therefore different velocities. As a consequence they need different times to reach x_c and hence their cross sections will be different. From the above equations a simple expression for the ratio of the cross sections of two isotopes results:

$$\frac{\sigma_1}{\sigma_2} = \left(\frac{\sigma_{ex}}{\sigma_1} \right)^{\sqrt{m_2/m_1} - 1} \tag{8a}$$

$$= \left(\frac{1}{P_d} \right)^{\sqrt{m_2/m_1} - 1}. \tag{8b}$$

The arguments which lead to this expression should be applicable for desorption as well as for the dissociation with the fragments retained on the surface because neither details of the potential curves nor the dependence of the lifetime on x enter. In both cases the essential point is the amount of energy transferred into motion along a reaction coordinate during the lifetime of an excitation. In the case of dissociation with the fragments retained on the surface it is the barrier height of this process which plays the role of the binding energy in stimulated desorption.

The only unknown and nonobservable quantity in Eq. (8a) is the excitation cross section σ_{ex}. Hence it can be determined from our data (Table II). For desorption the mass ratio is obviously 18:20. For the process, that becomes visible in the conversion feature, we assume that it is dissociation of H_2O into H + OH, and use a mass ratio of 1:2.[56] We then obtain, in both cases, an excitation cross section σ_{ex} of about 1×10^{-17} cm^2. The probability P_d is 1/400 for desorption and 1/7.1 for the conversion process. It should be noted that the error margin is rather large because of the form of Eq. (8b). A factor of 2 for the evaluation of the desorption data and 25% for the dissociation are certainly reasonable estimates. The last quantity P_d is independent from the above discussed question whether more than one molecule is converted by one dissociated H_2O molecule, whereas this ratio would directly enter into the calculation of the primary excitation cross section and reduce it proportionally. But even with these precautions the comparable primary excitation cross sections for both processes suggest, that a common initial excitation drives both processes, which had already been speculated above based on the rather similar change of cross sections from 5.0 to 6.4 eV excitation. Surprisingly quenching turns out to be less efficient for dissociation than for desorption, although it appears reasonable to assume that the OH bond energy will be higher than the H_2O desorption energy. It must therefore be concluded that energy transfer into the OH coordinate is more effective, which can perhaps itself be rationalized based on the light mass of the H atom.

The existence of the strong isotope effects is a clear evidence for the operation of strong quenching as considered in the MGR model. To our knowledge, this is the first time that it has been experimentally demonstrated in surface photochemistry. Only a process involving an excitation onto an excited potential which displaces the nuclei followed by rap-

TABLE II. Primary excitation cross section, σ_{ex}, and survival probabilities, P_d ($h\nu = 6.4$ eV).

	σ_1/σ_2 observed	m_1/m_2	σ_{ex} [10^{-18} cm^2]	P_d
Desorption	1.4	18/20	18.4	1/400
Conversion	2.2	1/2	9.6	1/7.1

id quenching so that only a minor fraction of excited molecules will desorb/dissociate can lead to such marked isotope effects.

The analysis of the isotope effects further indicates that both processes are direct and that energy transfer from one coordinate into another after deexcitation does not dominate. Especially H_2O desorption can not be caused by energy transfer from the OH vibration into the molecules surface bond. The OH vibration must be strongly excited in that fraction of H_2O molecules that fail to dissociate because of the quenching. Thus a distribution of vibrationally hot H_2O molecules results, from which desorption might occur by energy transfer from the intramolecular vibration to the surface–molecule bond. Assuming such an energy transfer mechanism the isotope effect for desorption would have to be analyzed taking the mass ratio 1:2 corresponding to the initial excitation that is quenched. Under this assumption, analysis leads to a small value, 1×10^{-19} cm^2, for the excitation cross section σ_{ex}. This value differs by 2 orders of magnitude from the value obtained analyzing the isotope effect in dissociation. Thus we arrive at a contradiction to the assumption made in this model that both processes originate from *one* excitation to a state only dissociative in the OH bond. We find that merely by assuming the most obvious mass ratios of 18:20 and 1:2 for desorption and dissociation, respectively, physically meaningful values for the primary excitation cross section and quenching probability are obtained. Hence the excited state must directly induce cleavage of the surface–molecule bond. But this can arise from either a repulsive potential function in the direction of the surface molecule bond or, in the sense of the Antoniewicz variant of the MGR process,[54] from a stronger molecule–surface attraction, leading to significant displacement towards the surface. In the latter deexcitation takes place over the repulsive branch of the ground state potential. The stronger attraction might well be due to the image charge potential induced by the transient H_2O^-. But at present our data do not allow to conclude which description is appropriate.

Based on the total quantum yield for desorption (5×10^{-5}), the absorptivity of Pd at 6.4 eV (0.63), and the excitation cross section σ_{ex} of 1×10^{-17} cm^2 it can be concluded that $\sim1\%$ of the photons absorbed by the metal results in one of these excitations. From these subsequent dissociation and desorption proceed with the probabilities P_d. Thus we obtain for the first time a detailed picture of the probabilities of the individual steps in this kind of processes. The excitation cross section derived from our measurements is also in the range of values known for the dissociative electron attachment resonances of gas phase H_2O.[57]

V. CONCLUSIONS

The results reported here can be summarized as follows:

(i) UV irradiation with 5.0 and 6.4 eV photons of a H_2O covered Pd(111) surface leads to desorption as well as dissociation of adsorbed molecules. Both processes share a common dependence on photon energy and are by about a factor of 25 more efficient for 6.4 eV excitation.

(ii) Time-of-flight spectroscopy shows that desorption is nonthermal with an average translational energy $\langle E_{trans}\rangle/2k$, of 600 K.

(iii) The photochemistry occurs preferentially for those molecules bound in the first layer (bilayer). Desorption from multilayers is an order of magnitude less efficient and leads to a smaller translational energy.

(iv) Both processes show marked isotope effects confirming that a description like in the MGR model is appropriate for these processes. The isotope effects are interpreted as being due to competition between quenching and mass dependent energy transfer into motion along the "reaction coordinate."

(v) Both observed processes might well be due to a common excitation which involves electron transfer from the metal to an adsorbed water molecule. This excited state must be dissociative in the OH bond but in the molecule–surface bond it can be either repulsive or, as proposed by the Antoniewicz model, stronger attractive.

ACKNOWLEDGMENTS

We thank G. Buntkowski for generously providing the D_2O used and X. -Y. Zhu for asking the awkward questions. J. M. W. acknowledges a senior scientist fellowship by the Alexander von Humboldt Stiftung.

[1] T. J. Chuang, Surf. Sci. Rep. **3**, 1 (1983).
[2] R. M. Osgood, Jr., Annu. Rev. Phys. Chem. **34**, 77 (1983).
[3] W. Ho, in *Desorption Induced by Electronic Transitions*, DIET IV, Springer Series in Surface Science (Springer, Berlin, 1990), Vol. 19, p. 48.
[4] P. Avouris and R. E. Walkup, Annu. Rev. Phys. Chem. **40**, 173 (1989).
[5] S. A. Costello, B. Roop, Z. M. Liu, and J. M. White, J. Phys. Chem. **92**, 1019 (1988); Z.-M. Liu, S. A. Costello, B. Roop, S. R. Coon, S. Akhter, and J. M. White, *ibid.* **93**, 7681 (1989); B. Roop, K. G. Lloyd, S. A. Costello, A. Campion, and J. M. White, J. Chem. Phys. **91**, 5103 (1989).
[6] E. P. Marsh, M. R. Schneider, T. L. Gilton, F. L. Tabares, W. Meier, and J. P. Cowin, Phys. Rev. Lett. **60**, 2551 (1988); E. P. Marsh, F. L. Tabares, M. R. Schneider, T. L. Gilton, W. Meier, and J. P. Cowin, J. Chem. Phys. **92**, 2004 (1990).
[7] F. Budde, A. V. Hamza, P. M. Ferm, D. Weide, P. Andersen, and H. J. Freund, Phys. Rev. Lett. **60**, 1518 (1988); P. M. Ferm, F. Budde, A. V. Hamza, S. Jakubith, G. Ertl, D. Weide, P. Andresen, and H. -J. Freund, Surf. Sci. **218**, 467 (1989).
[8] S. A. Buntin, L. J. Richter, R. R. Cavanagh, and D. S. King, Phys. Rev. Lett. **61**, 1321 (1988); S. A. Buntin, L. J. Richter, R. R. Cavanagh, and D. S. King, J. Chem. Phys. **91**, 6429 (1989).
[9] S. K. So, R. Franchy, and W. Ho, J. Chem. Phys. **91**, 5701 (1989).
[10] E. Hasselbrink, S. Jakubith, S. Nettesheim, M. Wolf, A. Cassuto, and G. Ertl, J. Chem. Phys. **92**, 3154 (1990).
[11] X. -Y. Zhu, S. R. Hatch, A. Campion, and J. M. White, J. Chem. Phys. **91**, 5011 (1989).
[12] L. Hanley, X. Guo, and J. T. Yates, Jr., J. Chem. Phys. **91**, 7220 (1989).
[13] M. Wolf, E. Hasselbrink, J. M. White, and G. Ertl, J. Chem. Phys. **93**, 5327 (1990).
[14] T. A. Germer and W. Ho, J. Chem. Phys. **89**, 562 (1988).
[15] J. R. Creighton, J. Appl. Phys. **59**, 410 (1986).
[16] J. R. Swanson, F. A. Flitsch, and C. M. Friend, Surf. Sci. **226**, 147 (1990).
[17] R. Gomer, in *Desorption Induced by Electronic Transitions*, DIET I, edited by N. H. Tolk, M. M. Traum, J. C. Tully, and T. E. Madey, Springer Series in Chemical Physics (Springer, Berlin, 1983), Vol. 24, p. 40.
[18] For a recent review, see P. A. Thiel and T. E. Madey, Surf. Sci. Rep. **7**, 211 (1987).
[19] S. Holloway and K. H. Benneman, Surf. Sci. **101**, 327 (1980).

[20]H. Itoh, G. Ertl, and A. B. Kunz, Z. Naturforschung **36a**, 347 (1981).
[21]K. Kretzschmar, J. K. Sass, A. M. Bradshaw, and S. Holloway, Surf. Sci. **115**, 183 (1982).
[22]D. Doering and T. E. Madey, Surf. Sci. **123**, 305 (1982).
[23]S. Anderson, C. Nyberg, and C. G. Tengstål, Chem. Phys. Lett. **104**, 305 (1985).
[24]P. Gurtler, V. Saile, and E. E. Koch, Chem. Phys. Lett. **51**, 386 (1977).
[25]M. Watanabe, H. Kitamora, Y. Nakai, *Proceedings of the IVth International Conference on VU Radiation Physics, Hamburg* (Pergamon, New York, 1974).
[26]K. Kobayashi, J. Phys. Chem. **87**, 4317 (1983).
[27]N. Nishi, H. Shinohara, and T. Okuyama, J. Chem. Phys. **80**, 3898 (1984).
[28]M. Wolf, S. Nettesheim, J. M. White, E. Hasselbrink, and G. Ertl, J. Chem. Phys. **92**, 1509 (1990).
[29]D. Burgess, Jr., P. C. Stair, and E. Weitz, J. Vac. Sci. Technol. A **4**, 1362 (1986).
[30]W. L. Gurthrie, T. -H. Lin, S. T. Ceyer, and G. A. Somorjai, J. Chem. Phys. **76**, 6398 (1982).
[31]R. H. Stulen and P. A. Thiel, Surf. Sci. **157**, 99 (1985).
[32]J. R. Creighton and J. M. White, Surf. Sci. Lett. **122**, L648 (1982).
[33]G. B. Fisher and B. A. Sexton, Phys. Rev. Lett. **44**, 683 (1980).
[34]C. Nyberg and C. G. Tengstål, J. Chem. Phys. **80**, 3463 (1984).
[35]E. M. Stuve, S. W. Jorgensen, and R. J. Madix, Surf. Sci. **146**, 179 (1984).
[36]*Physik Daten*, Vol. 18–1, edited by H. Behrens and G. Ebel (Fachinformationszentrum, Karlsruhe, 1981).
[37]M. Born and E. Wolf, *Principles of Optics* (Pergamon, Oxford, 1980).
[38]W. N. Hansen, J. Opt. Soc. Am. **58**, 380 (1968).
[39]L. C. Lee, J. Chem. Phys. **72**, 4334 (1980).
[40]M. Bowker, M. A. Barteau, and R. J. Madix, Surf. Sci. **92**, 528 (1980).
[41]C. E. Melton, J. Chem. Phys. **57**, 4218 (1972).
[42]D. S. Belić, M. Landau, and R. I. Hall, J. Phys. B **14**, 175 (1981).
[43]G. B. Fisher and J. L. Gland, Surf. Sci. **94**, 446 (1980).
[44]M. J. Campbell, J. Liesegang, J. D. Riley, R. C. G. Lecky, J. G. Jenkin, and R. T. Poole, J. Electron Spectrosc. Relat. Phenom. **15**, 83 (1979).
[45]I. N. Levine, *Quantum Chemistry*, 3rd ed. (Allyn and Bacon, Boston, 1983), pp. 242–442.
[46]C. R. Claydon, G. A. Segal, and H. S. Taylor, J. Chem. Phys. **54**, 3799 (1971).
[47]G. D. Kubiak, J. Vac Sci. Technol. A **5**, 731 (1987).
[48]T. L. Gilton, C. P. Dehnbostel, and J. P. Cowin, J. Chem. Phys. **91**, 1937 (1989).
[49]X. -Y. Zhu, J. M. White, M. Wolf, E. Hasselbrink, and G. Ertl (in preparation).
[50]R. N. Compton and L. G. Christophorou, Phys. Rev. **154**, 110 (1967).
[51]T. E. Madey, J. T. Yates, Jr., D. A. King, and C. J. Uhlander, J. Chem. Phys. **52**, 5215 (1970).
[52]W. Jelend and D. Menzel, Chem. Phys. Lett. **21**, 178 (1973).
[53]D. Menzel and R. Gomer, J. Chem. Phys. **41**, 3311 (1964).
[54]P. A. Redhead, Can. J. Phys. **42**, 886 (1964).
[55]P. R. Antoniewicz, Phys. Rev. B **21**, 3811 (1980).
[56]The same mass ratio results if the reduced masses of the H–OH or D–OD system are considered. Assuming a mass ratio of 18:20 for the conversion process leads to rather unphysical results with an excitation cross section σ_{ex} of 10^{-12} cm^2 and on the other hand a P_d of 10^{-6}, which is a contradiction to the observed quantum yield of 10^{-4} and the established single photon character of the process.
[57]L. G. Christophorou, D. L. McCorkle, and A. A. Christodoulides, in *Electron–Molecule Interactions and Their Applications*, Vol. 1 (Academic, Orlando, 1984).